Electronic Supplementary Information (ESI)

Creation of nanopores on graphene planes with MgO template for preparing high-performance supercapacitor electrode

Huanjing Wang, Xiuxia Sun, Zonghuai Liu and Zhibin Lei*

School of Materials Science and Engineering, Shaanxi Normal University, 199 South Chang'an Road, Xi'an, Shaanxi, 710062, China, Email: zblei@snnu.edu.cn;
Tel: 86-29-81530810; Fax: 86-29-81530702

*Corresponding Authors:
Prof. Zhibin Lei, School of Materials Science and Engineering, Shaanxi Normal University, 199 South Chang'an Road, Xi'an, Shaanxi, 710062, China. Email: zblei@snnu.edu.cn; Tel: 86-29-81530810; Fax: 86-29-81530702

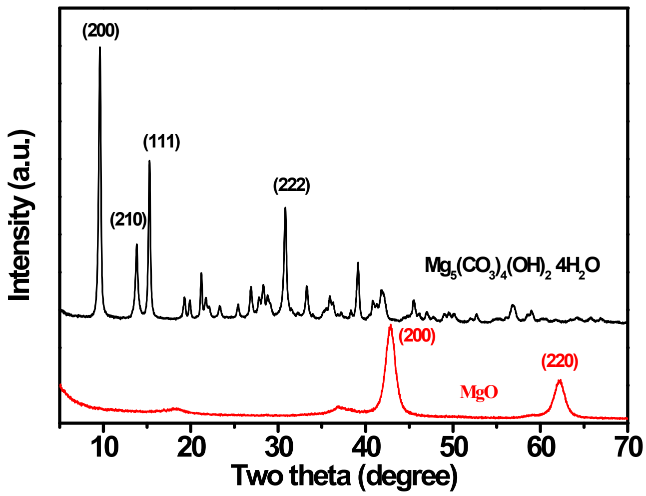

Fig. S1. XRD patterns of magnesium hydroxide carbonate and magnesium oxide.

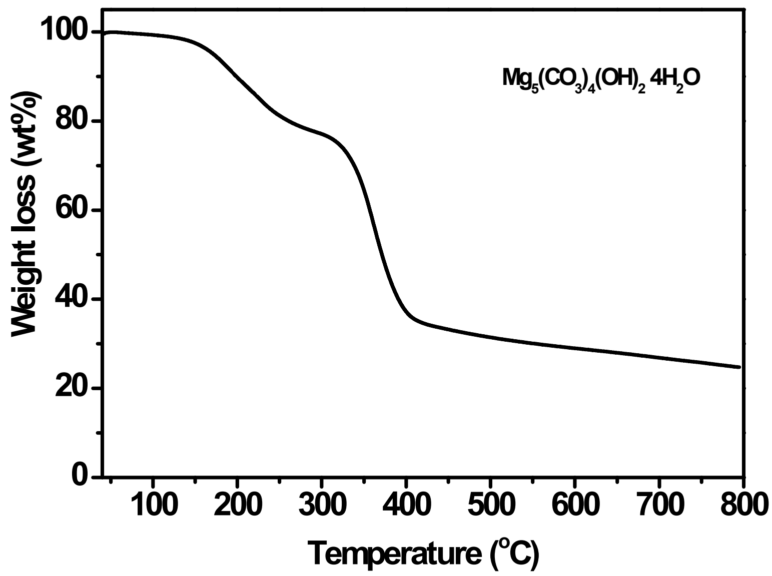

Fig. S2 TGA curve of magnesium hydroxide carbonate in flowing air.

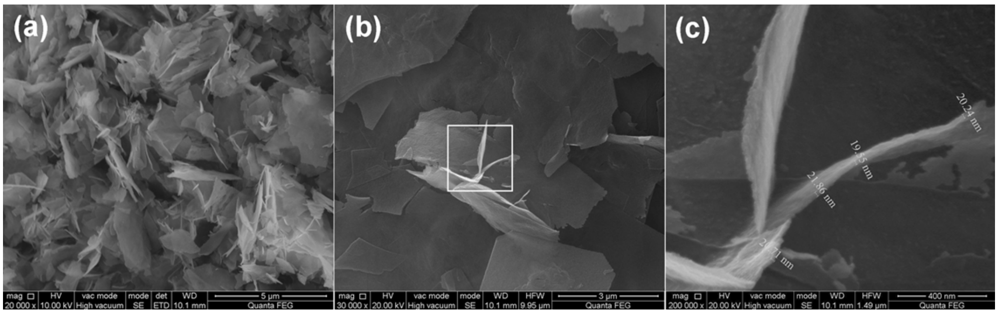

Fig. S3. SEM images of MgO flake with different magnifications. The thickness of MgO flake is estimated to be 20 nm (c).

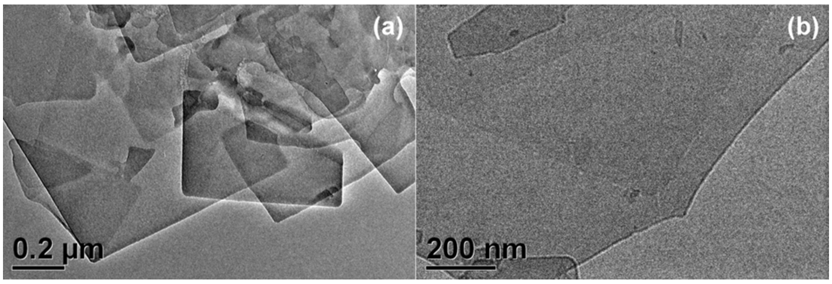

Fig. S4. TEM images of $Mg_5(CO_3)_4(OH)_2 \cdot 4H_2O$ prepared by the co-precipitation reaction of $Mg(NO_3)_2 \cdot 6H_2O$ with urea at 95 °C

Table S1 Structure parameters of MgO precursor and the porous graphene

Sample	Specific surface area (m^2 g^{-1})	Pore volume (cm^3 g^{-1})
$Mg_5(CO_3)_4(OH)_2 \cdot 4H_2O$	25	0.11
MgO	41	0.16
Graphene/MgO	100	0.20
Graphene	1754	2.81

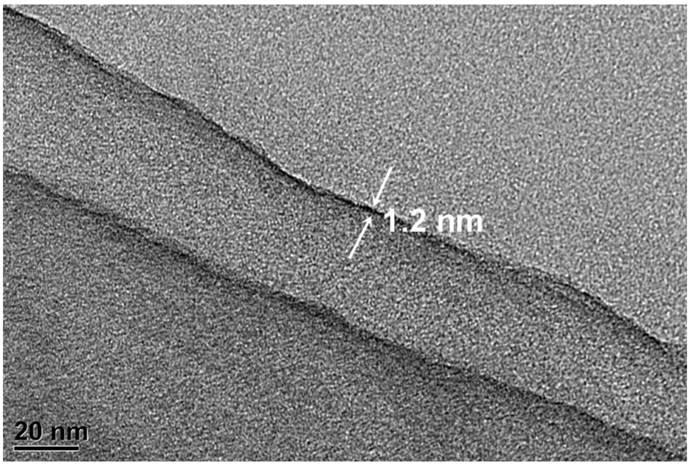

Fig. S5. HRTEM images of porous graphene with a sheet thickness about 1.2 nm.

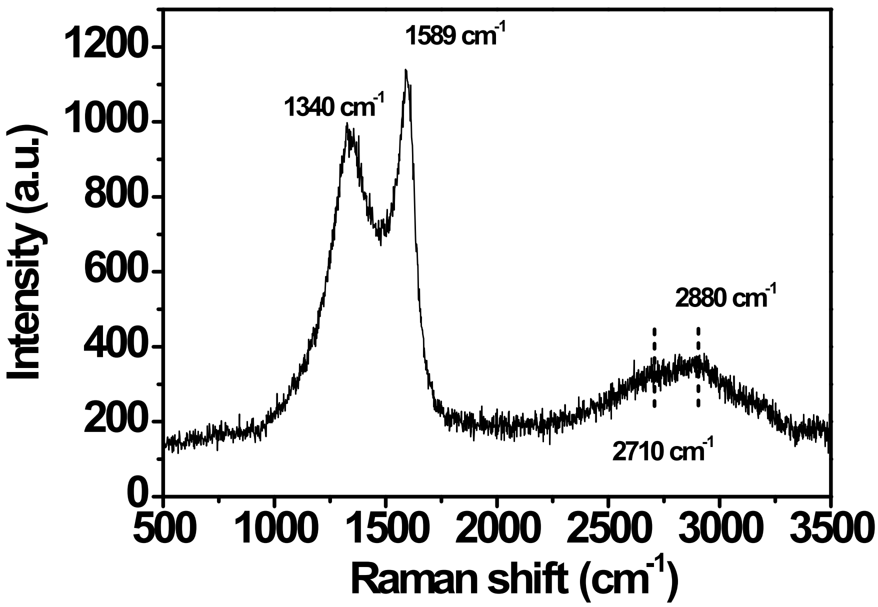

Figure S6 Raman spectrum of the porous graphene.

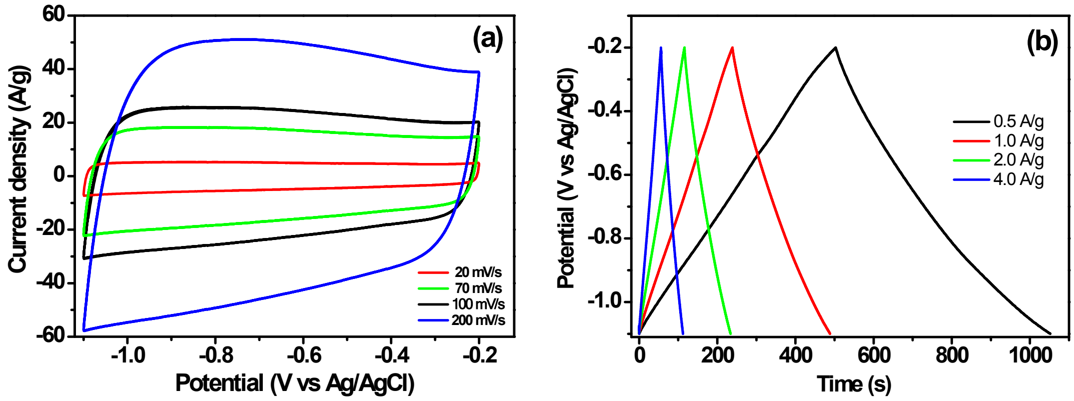

Figure S7. CV (a) and galvanostatic charge-discharge curves (b) of porous graphene electrode at different current densities. Data obtained from three-electrode cell with 6.0 mol L^{-1} KOH as aqueous electrolyte.

Table S2 Comparative electrocapacitive performances of graphene materials prepared by various methods

Samples	Synthesis methods	Specific capacitance (F/g)	Electrolyte	Energy density (Wh/kg)	Power density (kW/kg)	Reference
3D-GFs	Soft template	226	H_2SO_4 (1.0 M)	–	–	[1]
RGO	Chemical reduction by urea and N_2H_4	218-255	KOH (6.0 M)	5.8	10	[2, 3]
3D a-MEGO	KOH activation	165	$BMIMBF_4$/AN	70	–	[4]
Graphene hydrogel	Chemical reduction by glutathione	157.7	Na_2SO_4 (0.5 M)	5.5	< 10	[5]
3D graphene hydrogel film	Hydrothermal reduction	186-196	H_2SO_4-PVA	–	–	[6]
RGO	Thermal reduction	96	H_2SO_4 (5.0 M)	12.8	160	[7]
3D macroporous graphene frameworks	Template by polystyrene spheres	202	Na_2SO_4 (1.0 M)	5.5	10	[8]
3D HPG	Heating ion-exchanged resin	178	$TEMABF_4$/PC	38	260	[9]
Non-stacked RGO	Anti-solvent method	236.8	KOH (6.0 M)	–	–	[10]

Curved graphene	Thermal reduction	100-250	EMIMBM$_4$ (0-4.0 V)	85.6	10	[11]
Chemically modified	Chemical reduction of GO	135	KOH (5.5 M)	–	–	[12]
graphene	by hydrazine	99	TEABF$_4$/AN (1.0 M)	–	–	
Graphene-CMK-5	Electrostatic assembly	144.4	EMIMBM$_4$ (0-3.5 V)	60.7	10	[13]
Restacking-inhibited 3D	Thermal reduction of	210	LiPF$_6$/EC/DEC	–	–	[14]
RGO	melamine-mediated GO					
asMEG-O	Activation by KOH	174	BMIMBF$_4$/AN (1:1)	74	338	[15]
Porous activated RGO	Activation by KOH	120	TEABF$_4$/AN (1.0)	26	500	[16]
Porous graphene	CVD and template	303	KOH (6.0 M)	6.5	12.6	This work
			TEABF$_4$/AN (1.0)	29.6	21.6	

References and Notes:

EMIMBF$_4$: 1-ethyl-3-methylimidazolium tetrafluoroborate ionic liquid electrolyte

BMIMBF$_4$/AN: 1-butyl-3-methyl-imidazolium tetrafluoroborate dissolved in acetonitrile.

(1) Z.-S. Wu, Y. Sun, Y.-Z. Tan, S. Yang, X. Feng and K. Müllen, *J. Am. Chem. Soc.*, 2012, **134**, 19532.

(2) Z. Lei, L. Lu and X. S. Zhao, *Energy Environ. Sci.*, 2012, **5**, 6391.

(3) Z. B. Lei, N. Christov and X. S. Zhao, *Energy Environ. Sci.*, 2011, **4**, 1866.

(4) Y. W. Zhu, S. Murali, M. D. Stoller, K. J. Ganesh, W. W. Cai, P. J. Ferreira, A. Pirkle, R. M. Wallace, K. A. Cychosz, M. Thommes, D. Su, E. A. Stach and R. S. Ruoff, *Science*, 2011, **332**, 1537.

(5) H. Gao, F. Xiao, C. B. Ching and H. Duan, *ACS Appl. Mater. Interfaces*, 2012, **4**, 2801.

(6) Y. Xu, Z. Lin, X. Huang, Y. Liu, Y. Huang and X. Duan, *ACS Nano*, 2013, **7**, 4042.
(7) H. Zhang, V. V. Bhat, N. C. Gallego and C. I. Contescu, *ACS Appl. Mater. Interfaces*, 2012, **4**, 3239.
(8) B. G. Choi, M. Yang, W. H. Hong, J. W. Choi and Y. S. Huh, *ACS Nano*, 2012, **6**, 4020.
(9) Y. Li, Z. Li and P. K. Shen, *Adv. Mater.*, 2013, **25**, 2474.
(10) Y. Yoon, K. Lee, C. Baik, H. Yoo, M. Min, Y. Park, S. M. Lee and H. Lee, *Adv. Mater.*, 2013, **25**, 4437.
(11) C. Liu, Z. Yu, D. Neff, A. Zhamu and B. Z. Jang, *Nano Lett.*, 2010, **10**, 4863.
(12) M. D. Stoller, S. Park, Y. Zhu, J. An and R. S. Ruoff, *Nano Lett.*, 2008, **8**, 3498.
(13) Z. Lei, Z. Liu, H. Wang, X. Sun, L. Lu and X. S. Zhao, *J. Mater. Chem. A*, 2013, **1**, 2313.
(14) J. H. Lee, N. Park, B. G. Kim, D. S. Jung, K. Im, J. Hur and J. W. Choi, *ACS Nano*, 2013, **7**, 9366.
(15) T. Kim, G. Jung, S. Yoo, K. S. Suh and R. S. Ruoff, *ACS Nano*, 2013, **7**, 6899.
(16) L. L. Zhang, X. Zhao, M. D. Stoller, Y. Zhu, H. Ji, S. Murali, Y. Wu, S. Perales, B. Clevenger and R. S. Ruoff, *Nano Lett.*, 2012, **12**, 1806.

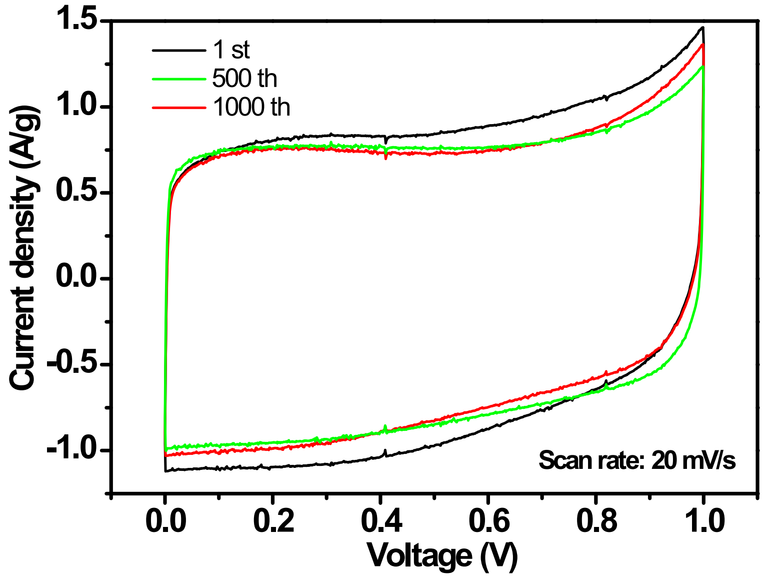

Figure S8. CV curves of porous graphene-based two-electrode capacitor during the 1000 continuous cycling with 6.0 mol L^{-1} KOH as aqueous electrolyte.

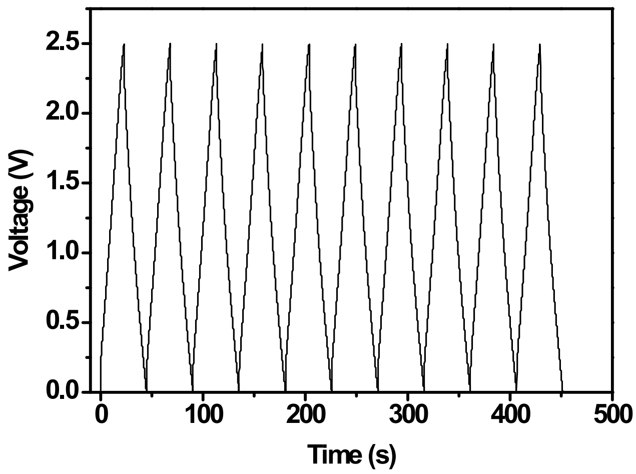

Figure S9. The last ten cycles in 1000 galvanostatic charge-discharge cycles of porous graphene two-electrode capacitor measured at current density of 3.0 A g^{-1} in 1.0 mol L^{-1} $TEABF_4$/AN electrolyte.